TECHNICAL MEMORANDUM

790

Improving CAMS biomass burning estimations by means of the Global ECMWF Fire Forecast system (GEFF)

Francesca Di Giuseppe [1] and Samuel Rémy [2] and Florian Pappenberger[1] and Fredrik Wetterhall[1]

[1]European Centre for Medium-Range Weather Forecasts, Reading, UK
[2] Laboratoire de Météorologie Dynamique, CNRS/UPMC, Paris, France

Published in the Journal of the Applied Meteorology and Climatology

August 22, 2017

European Centre for Medium-Range Weather Forecasts
Europäisches Zentrum für mittelfristige Wettervorhersage
Centre européen pour les prévisions météorologiques à moyen terme

Series: ECMWF Technical Memoranda

A full list of ECMWF Publications can be found on our web site under:
http://www.ecmwf.int/en/research/publications

Contact: library@ecmwf.int

Abstract

The atmospheric composition analyses for the European Copernicus Atmosphere Monitoring Services (CAMS) relies on biomass burning fire emission estimates from the Global Fire Assimilation System (GFAS), which converts Fire Radiative Power (FRP) observations from MODIS satellites into smoke constituents. In case of missing observations GFAS relies on persistence, meaning that values of FRP observed the previous day are progressed in time until an observation is obtained. The statistical consequence of this assumption is an overestimation of fire duration which translates into an overestimation of fire emissions.

Also CAMS assumes persistence; meaning that biomass burning emissions calculated by the GFAS analysis are kept invariant during the forecast. This assumption is simple and practical in the absence of a dynamical fire model that could predict fire emissions evolution linked to the dynamical evolution of weather conditions and the available vegetation fuel. Nevertheless it can produce unrealistic aerosols and chemical predictions.

Since 2012 ECMWF has been involved in the development of the modeling components of the European Forest Fire Information System (EFFIS) which is currently being developed in the framework of the Copernicus Emergency Management Services to monitor and forecast fire danger in Europe. Under the EFFIS umbrella, ECMWF has developed the Global ECMWF Fire Forecast (GEFF) system which models fire danger conditions and fire behaviors using the ECMWF Ensemble Prediction System (EPS).

Therefore, as an improvement to the CAMS systems we propose the synergistic use of the already existing GEFFs products to bring the benefit of a fire modeling component into the fire emission estimates. We propose the introduction of a modulation factor, $\mathscr{M}$, to be applied to the emission sources during the forecast integration where $\mathscr{M}$ is predicted from the daily variability of the FWI.

GFAS performance indicates that the FWI based model is a better tool than persistence to infer FRP at missing observation locations. Similarly, in CAMS, the use of the FWI based modulation factor has also a positive impact on the forecasted emissions.

1 Introduction

For some chemical compounds such as carbon dioxide and monoxide, the total annual emission from biomass burning is comparable to what is emitted from anthropogenic sources (Crutzen et al., 1979). Chemical fluxes arising from fires are therefore a non negligible source of emissions in forecasting system of the atmospheric composition, such as the European Copernicus Atmosphere Monitoring Services (CAMS). Since 2012, the Global Fire Assimilation System (GFAS) is a CAMS operated off-line analysis system which estimates fire emissions by converting the energy released during fire combustion into gases and aerosol fluxes (Di Giuseppe et al., 2016; Kaiser et al., 2012).

GFAS uses observations of fire radiative power (FRP) from two MODIS sensors on board of the Aqua and Terra satellites (Kaufman et al., 2003). FRP measures the heat power emitted by fires as a result of the combustion process and is directly related to the total biomass combusted (Wooster et al., 2005). Using land-use dependent conversion factors, GFAS converts FRP into emission estimates of 44 smoke constituents, such as CO, CO_2, CH_4, black-carbon and organic matter components of the aerosols (Kaiser et al., 2012). These fluxes are then ingested in the model managed by the CAMS to produce daily forecast of chemical composition at the global scale. GFAS converts MODIS observations into emissions and does not explicitly forecast fire behavior or fire evolution. Also the model operated by the CAMS does not include a fire model component to predict the evolution of fire emissions. The emissions estimated at the initial analysis time by the GFAS are kept constant during the five-day forecast (Flemming et al., 2015).

Weather is the most important factor in modulating fire intensities where fuel is available (Flannigan et al., 2009). Weather also affects the fire emissions by changing the fuel moisture content (Di Giuseppe et al., 2016; French et al., 2011, 2014). A simple functional link between weather and fire is provided by the class of fire danger models as they describe the impact that atmospheric conditions have on fuel availability. However simple they tend to perform very well where biomass moisture is a limiting factor to fire sustainability as in temperate and tropical rain-forests, where fuel is abundant. Their performance instead deteriorate in fuel-limited ecosystems such as semi-arid, tropical and temperate savannas and in the Mediterranean. Here vegetation conditions are persistently hot and dry but ignitions and fuel availability is scarce except on rare and difficult to predict occasions (Di Giuseppe et al., 2016). Among others the Canadian Fire Weather Index (FWI) is one of the most commonly used fire danger rating system. It was developed as a metric for fire danger in a standard jack pine stand *Pinus banksiana* typical of Canadian forests (Van Wagner et al., 1974) and it only uses meteorological inputs, such as air temperature, wind speed, relative humidity and 24 hours cumulative rainfall (Van Wagner et al., 1987). The relative simplicity of its formulation has contributed to its popularity and has resulted in its extensive use in other climate regions very dissimilar to Canada (Taylor and Alexander, 2006) such as Australia (Cruz and Plucinski, 2007), New Zealand and Malaysia (Taylor and Alexander, 2006) and Indonesia(De Groot et al., 2007; Field et al., 2009). The FWI has shown to provide useful information worldwide (Di Giuseppe et al., 2016).

In this paper we propose the use of the Fire Weather Index to predict changes in fire emissions during the CAMS forecast building on the idea that there is a strong link between emissions released during fires and the weather. Linear changes in the FWI are translated in linear changes in fire emission; this assumption substitutes the previously adopted persistence assumption in which no evolution takes place from the initial analysis date. The new method is assessed using 5 month of daily forecasts from June to October 2015. As only limited information is available on the mass fluxes released into the atmosphere during fires, the validation of the new scheme is performed indirectly by looking at the overall quality of the forecast from the point of view of aerosol prediction.

2 Method

FRP observations from MODIS are available at 1km resolution. GFAS processes these observations by interpolating them on to a 0.1 degree regular grid and then converting the average FRP value into dry matter, $\bar{\rho}$, following Wooster et al. (2005). The conversion into emission rates for 44 constituents, $\mathscr{E}_i$, is performed using the simple formulation

$$\mathscr{E}_i = \bar{\rho} \cdot \mathscr{X}_i \tag{1}$$

where $\mathscr{X}_i$ are the land-use dependent conversion coefficients from Heil et al. (2010) expressed in g(species)Kg^{-1}(dry matter). Then, $\mathscr{E}_i$ is the mean daily emission for the given specie expressed in grams.

The CAMS uses the emissions, $\mathscr{E}_i$, available at the analysis time, t_0, as to initialize the chemical constituents arising from the biomass burning process (Flemming et al., 2015). The emissions, $\mathscr{E}_i$, are persistent during the 5-day forecast. Keeping the emission constant is a practical choice as a fire model is not available. Yet it can lead to severe overestimations of the biomass burning contribution especially in case of short-lived events. As an improvement we propose the introduction of a modulation factor to change the fire emissions on the base of weather conditions. The function chosen is a linear function of daily changes of FWI (Stocks et al., 1989; Van Wagner, 1985; Van Wagner et al., 1987). FWI was chosen as it is directly related to the fire intensity, i.e. the energy released during the biomass burning process (Van Wagner et al., 1987). Therefore the assumed link between the FWI and the fire emission is that the higher the FWI, the higher will be the fuel consumption hence the higher the emissions.

The FWI calculation is performed in two steps. In the first step atmospheric temperature, humidity, precipitation and wind modulates the fuel moisture content of three surface fuel components representative of typical fuel beds in a boreal forest. In the second step the fuel state is used to calculate two fire behavior indices; the rate of fire spread which mostly depends on the wind and the total fuel availability for combustion. The combination of these two latter indexes provides a unit-less index of general fire intensity potential, generally referred to as Fire Weather Index (Stocks et al., 1989; Van Wagner, 1985). FWI calculations are available daily through the Global ECMWF Fire Forecast (GEFF) system (Di Giuseppe et al., 2016). To take into account uncertainties in the fire indexes due to uncertainties in the weather parameters, GEFF produces an ensemble of values using the 51 weather forecast realization of ECMWF ensemble forecasting system (Buizza et al., 1999). Forecasts for temperature, humidity, wind and precipitation undergo a temporal interpolation to local noon (see for details Di Giuseppe et al. (2016)), which then are used as atmospheric forcing for the FWI forecasts. The ensemble mean is assumed to be the best FWI estimation.

The effect of a change in weather conditions on fire emissions in the proposed model is calculated as the daily change in FWI. A modulation factor, $\mathscr{M}$, is defined as:

$$\mathscr{M}(t) = \frac{FWI(t) - FWI(t_0)}{FWI(t_0)} \tag{2}$$

where t is the forecast time. Since FWI is a daily value, t has lead times between 1 and 5 days. The initial condition, t_0=0, is the starting day of the forecast, also referred to as analysis time. This corresponds to the day at which GFAS emissions, $\mathscr{E}_i(t_0)$, are calculated from the FRP observations. For convenience, the daily value of $\mathscr{M}$ is scaled to provide the relative change of FWI with respect to this initial day, FWI(t_0). During the CAMS integration the daily fire emissions change accordingly to equation 3

$$\mathscr{E}_i(t) = \mathscr{E}_i(t_0) * (1 + \mathscr{M}(t)) \tag{3}$$

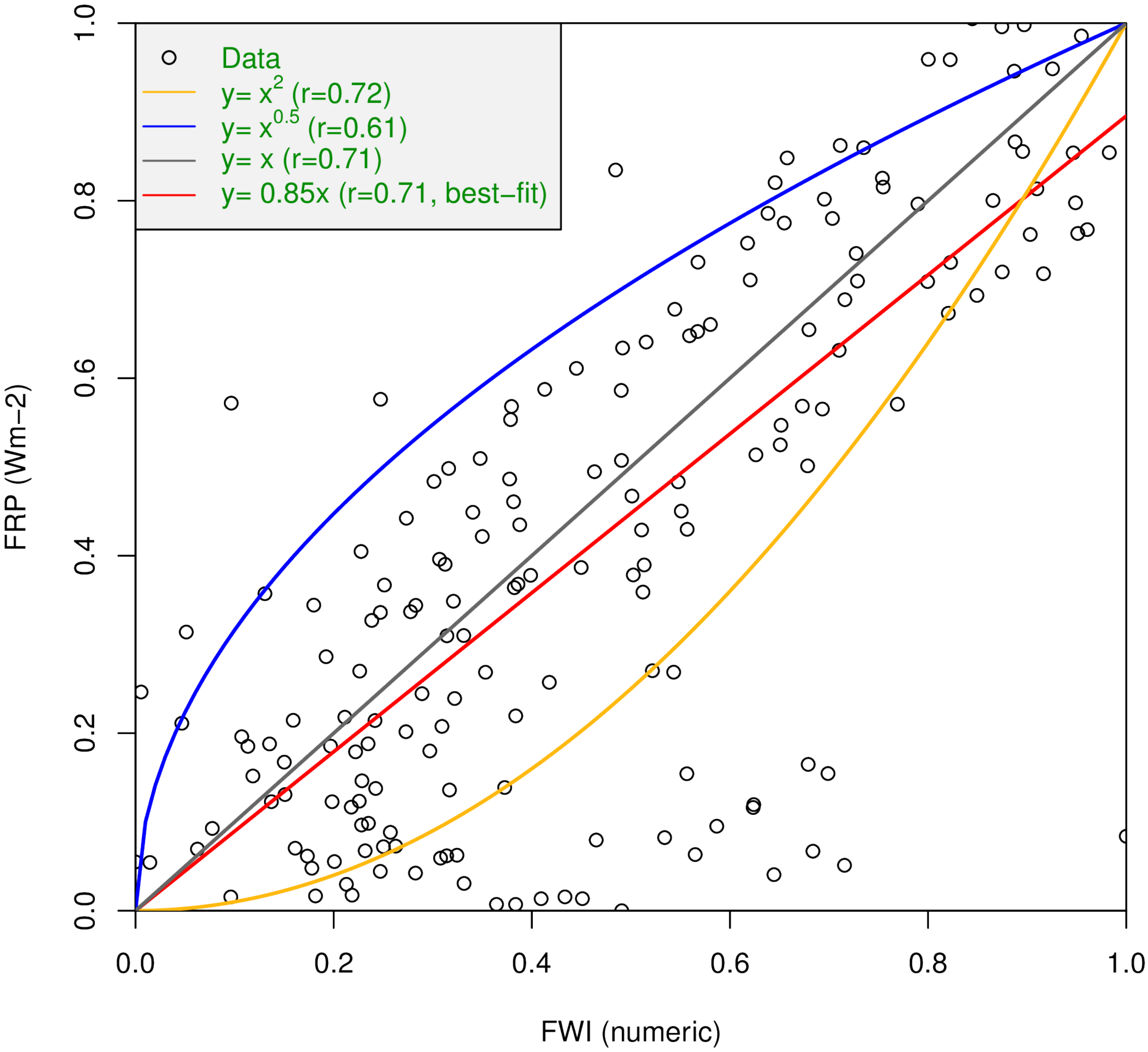

Figure 1: Relationship between FRP and FWI. The analysis is performed for 5 months and using only data for which $FRP > 0.5Wm^{-2}$. Several functional dependency are shown with their regression coefficients.

By substituting equation 2 in equation 3 it is clear that linear increments in the FWI are transformed into linear increments in emissions for each of the constituents. The assumption of linearity between FWI and the emissions has been verified looking at the relationship between FWI and FRP, where FRP values are themselves linearly related to the emissions. Figure 1 takes into account all $FRP > 0.5Wm^{-2}$ data points observed by MODIS (AQUA+TERRA) during 5 months from June to October 2015 and the corresponding FWI calculated from the GEFF. Data have been aggregated over a regular 9 km grid and three functions were tested 1. The linear model has similar correlation coefficient than the quadratic model and was chosen because of its simplicity.

Since $\mathscr{M}$ measures changes in fire danger conditions and not fire activities, it is defined for locations where fires are not occurring, i.e where observed FRP=0. These locations are not relevant in our application and are therefore masked out. Also, when FWI(t_0)=0, $\mathscr{M}(t)$ becomes undetermined at all times. In these rare cases the system reverts to the persistence assumption and $\mathscr{E}_i(t) = \mathscr{E}_i(t_0)$, $\forall$ t. However, Di Giuseppe et al. (2016) showed that globally observed fires associated to zero FWI value are extremely rare event with a probability of less than 1%.

Since FWI is positive defined and open ended, $\mathscr{M}$ can in theory vary in the interval $[-\infty;+\infty]$. This could lead to unrealistic modifications of the biomass burning emissions during the forecast. However, the FWI formulation has a strong build-up component through the drought code (Van Wagner, 1985) which is a smooth function of time that prevents large daily variations in FWI for a given location. $\mathscr{M}(t)$ is in practice constrained into a physically meaningful range of values and no rescaling was found necessary (see figure 2).

In summary, even if $\mathscr{M}(t)$ cannot be considered a full dynamical fire model with an interactive vegetation, it is a direct function of temperature, relative humidity, precipitation and wind through the FWI formulation. It therefore provides a physical base to simulate the emission evolution which also is consistent with the meteorology used by the CAMS chemical transport model.

3 Experiment set-up

To understand the impact of the fire emission modification in the CAMS some extensive fire events in 2015 were analyzed. 2015 was characterized by a strong El Niño which favored extensive fires in Indonesia in the autumn (El Niño fire section in the BAMS state of the climate 2015). The fires in Alaska were also particularly severe in June and July. A series of experiments covering both events were performed using an experimental version of the CAMS model which releases biomass burning aerosol emissions at an injection height computed by a plume rise model that has recently been embedded into GFAS (Rémy et al., 2017). There are however significant uncertainties associated with these injection height estimates, which has an impact on the forecasted plume. Two different runs were carried out to cover the Alaska fires in June-July 2015, and fires in Indonesia in September-October 2015. The control run uses the standard GFAS v1.2 configuration of Kaiser et al. (2012) where persistence is assumed during the 5-day forecast integration. This experiment is simply flagged as control (CTRL). The second experiment uses the GFAS v1.2 configuration but applies the modification explained in the previous section where the emissions are modulated by the FWI function. This experiment is tagged as FWI.

As a benchmark model simulation we also use the CAMS interim reanalysis dataset, ”CAMSiRA”, in which, among other observations, fire emissions are constrained to the observed GFAS values (Flemming et al., 2017). CAMSiRA comprises 6-hourly reanalysis of atmospheric composition for the period 20032015. It has an horizontal resolution of about 110 km on a reduced Gaussian grid and a vertical discretization of 60 levels from the surface to a model top of 0.1 hPa. The most relevant differences with the CTRL and FWI experiments is that CAMSiRA uses an older model version then the operational model and several observations are assimilated during the reanalysis integration. Total columns of carbon monoxide from the Measurements Of Pollution In The Troposphere (MOPITT) instrument (Deeter et al., 2003), MODIS AOD, and several ozone total column and stratospheric profile retrievals constrain the values of the AOD fields. Therefore, differences between the reanalysis, the CTRL and the FWI cannot be attributed to the different treatment of the fire emissions alone. Still, the comparison help sizing the improvement provided by the FWI implementation.

Two horizontal and vertical resolutions were tested. The high resolution experiment has a T_L1279 horizontal spectral resolution which corresponds to a grid-box size of about 9km and has a 137 vertical hybrid sigma-pressure levels. Experiments at the operational CAMS resolution T_L255 (which corresponds to a grid-box size of about 80km) and 60 vertical hybrid sigma-pressure levels were also performed. Table 1 summaries the experiment set-up.

Table 1: Summary of experiment set-up. T_L represents the spectral truncation of the CAMS model and defines the horizontal resolution. This representation is used in the model to compute some horizontal derivatives and for the implicit computations.

EXP-ID	RES	Description
CTRL	HRES= T_L1279 LRES= T_L255	GFAS v1.2 / CAMS model version CY41R1 using the operational configuration. Fire emissions calculated by GFAS at the analysis time t_0 are kept constant during the 5 days of the CAMS forecast.
FWI	HRES= T_L1279 LRES= T_L255	GFAS v1.2 / CAMS model version CY41R1 using the modified configuration. Fire emissions calculated from GFAS at the analysis time, t_0 are modulated by changes in the FWI during the 5 days of the CAMS forecast.
Reanalysis	HRES= Not available LRES= T_L159	GFAS v1.2 / CAMS model version CY40R2. Fire emissions from GFAS are continuously assimilated into CAMS.

4 Results

4.1 Modulation factor behavior

FRP changes due to the introduction of the modulation factor are shown as the global probability density function (PDF) of $\mathscr{M}$ as a function of forecast time (figure 2). Emissions changes take place only in the FWI experiment and $\mathscr{M}$ is zero at all lead times in the control experiment (CTRL). The PDF comprises data for 154 starting dates and only for observed fire locations, where $FRP > 0$ at t=t_0. 95 % of the forecasted increments are in the range [-0.4 ; +0.4]. The distribution is centered around zero for all the forecast lead times (maximum bias -0.02). This is a very desirable property of the modulation factor as it is not justified the positive or negative bias into the forecasted emissions as a function of lead time. Numerically, $\mathscr{M}$ could occasionally assume extremely large positive and negative values in the tails of the distribution. The range of $\mathscr{M}$ is cropped to $[-0.4;+0.4]$ to avoid these cases in the forecast experiments.

Daily variations in FWI translate into $\mathscr{M}$ increments which are in a reasonable range at all lead times (figure 2). It is more challenging to verify if these increments are also reducing model errors when compared to observations given the shortage of measurements of fire emissions. However, when MODIS FRP observations are available, they can be compared to the forecasted FRP (figure 3). FRP span a vast range of values with mean 0.7 Wm^{-2} and 3 Wm^{-2} standard deviation (not shown). By assuming persistence from the previous day produces an increase in the assimilated fire radiative power that is on average 0.14 Wm^{-2}, 20 % higher than what observed. This bias is reduced to -0.06 Wm^{-2} at lead time 1 day and to -0.07 Wm^{-2} at lead time 5 days with the application of the modulation factor.

One interesting aspect is that positive biases are reduced more than negative ones. This behavior can be explained noticing that FWI, by using FWI values only when fire events are observed, the FWI distribution is conditionally sampled towards high values (Di Giuseppe et al., 2016). This is evident from figure 4 where the PDF of the normalized FWI at the analysis time (t_0) is shown. The vast majority of

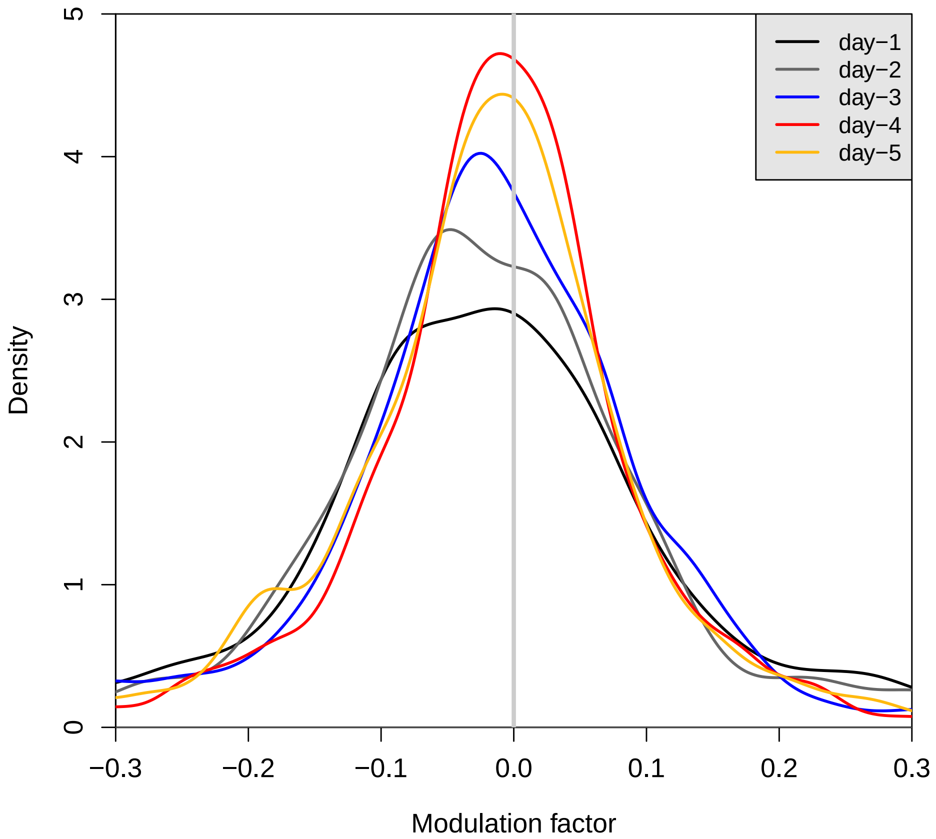

Figure 2: Probability distribution function for the modulation factor, $\mathcal{M}$. The PDF includes all data obtained during the five months of the validation period.

FWI values are above the upper quartile ($>$ 75%) as one would expect. From figure 4 it is also clear that FWI reaches an asymptotic high value above which FWI increase is limited. However precipitation and humidity rises can produce a large FWI decrease which will translate to large negative value for the modulation factor. Despite this asymmetric behavior the error in FRP is highly reduced (mean bias = 0.16 Wm^{-2}).

4.2 Case studies

The Indonesian fires in 2015 extended to vast areas and were long-lived. The fires started in early September and only diminished in intensity by the beginning of November, thanks to the onset of seasonal precipitation. Human caused fires are not unusual in Indonesia mostly due to logging practices (Field et al., 2009; Spessa et al., 2015). Further, in 2015 the effect of human practice was amplified by the extensive and persistent droughts which affected parts of south-east Asia. This contributed to making the situation far worse than usual. Areas of forest, particularly on peat, that are normally too wet to burn turned into fires, leading to extremely widespread and severe burning activities. The fire season began in August and by September, much of Sumatra, Kalimantan, Singapore, and parts of Malaysia and Thai-

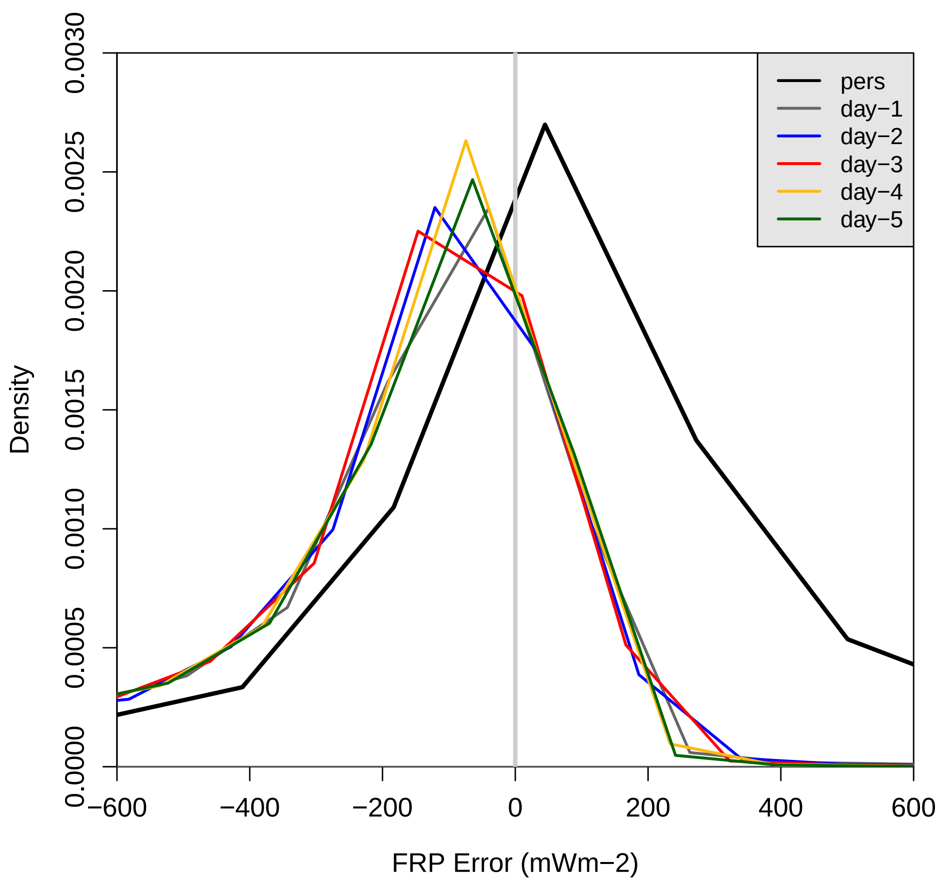

Figure 3: Probability distribution function of model errors. The model error is expressed as forecast minus observed Fire Radiative Power (FRP). Different curves refers to different lead times.

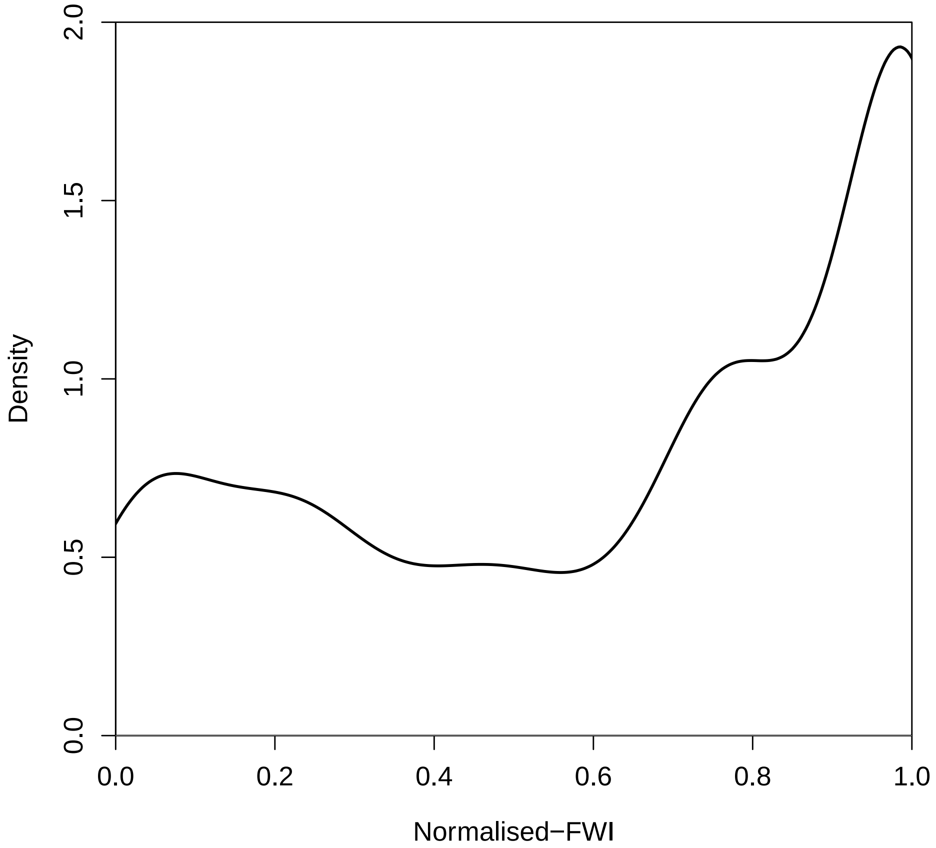

Figure 4: Probability density function of the normalized FWI at the analysis time, t_0. Only points where a fire is detected by MODIS are considered. The FWI normalization was performed using an historical time-series of FWI values for the period 1980-2014, then estimating the cumulative distribution function and its inverse (see Di Giuseppe et al. (2016) for more details). For example, a value of 0.5 identifies points that have a 50% chance to occur.

land were covered in thick smoke, which affect the respiratory health of millions of people (Marlier et al., 2013). At its peak, visibility was reduced to less than 10 % of normal in places, similar to conditions in El Niño years (Wang et al., 2004). Large parts of Borneo could not be seen from space. Preliminary estimates suggest that greenhouse gas emissions from the burning exceeded those of Japans mean annual fossil fuel emissions (Benedetti et al., 2016). The remnant pollution stretched halfway around the equator even after the worst of the fire was over.

In summer 2015 intense wild-fires also affected Alaska. Due to the unusually warm conditions fires burned all the way down to the mineral soil. When this occurs the frozen ground loses its insulation and the permafrost can thaw, sometimes so much that the ground sinks and becomes bumpy and hilly as it loses solid ice mass. The fire characteristics in boreal forests are very much different from the fires in southeast Asia and the ones in Indonesia. Since these latter burn sustained by an almost unlimited peat fuel availability they tend to be long lasting and of low intensity while forest fires are usually short lived and intense. The boreal forest zone consists of a mixture of conifers (white and black spruce, jack pine, tamarack, and balsam fir) for which the FWI model was specifically calibrated, we therefore expect the FWI to be a better predictor of fire danger for this vegetation cover.

To gain an understanding of how the new modulation factor modifies the CAMS emissions it is useful to consider the Alaska fire event in 2015. This was a collection of intense but localized fires which had their maximum of intensity on the 07 of July 2015 which was taken as the reference forecast. This study concentrates on the first 48 hours of forecast, but the same results were found valid at all lead times. By analyzing the difference between the FRP observed at t_0 (07 of July 2015) and t_0+48hr (09 of July 2015) (figure 5) it is clear that a decrease in fire activity was recorded.

The modulation factor $\mathscr{M}$ is also negative showing how the decrease in fire activity was correctly predicted by the change in FWI (figure 6). The magnitude of the modulation was stronger and more localized in the high resolution run (figure 6-B) in comparison with the simulation performed at the operational CAMS resolution (figure 6-A). The spatial localization of fires was also improved by the high resolution experiment.

As the modulation was negative at t_0+48h, also the forecasted aerosol emissions were decreased in the experimental run when compared with the standard CAMS configuration that uses persistence at all lead times (figure 7). The effect is remarkable in the high resolution experiment but becomes negligible at the standard CAMS resolution (not shown) as a consequence of the lower $\mathscr{M}$ values.

Given the scarcity of observations, it is challenging to verify if this reduction is also improving CAMS model errors. An encouraging result is nevertheless provided by the comparison with the AERONET station (Holben et al., 1998) at Bonanza Creek [lon= -142.379W; lat=64.997N] which is in the middle of the fire event and provides measurements of aerosol optical depth at 0.55 microns which can be compared with the model simulations (figure 8).

The analysis of the Alaska fire allows for a detailed understanding of how the introduction of $\mathscr{M}$ works to modulate emissions during the forecast integration. Being an isolated event it does not provide strong statistical evidence of the added benefit.

To understand the potential impact of $\mathscr{M}$ on a global scale also the 2015 Indonesia fires were analyzed. Fires were very extensive covering most of Indonesia and were so persistent that they produced a significant increase in the global aerosol emissions for that year Benedetti et al. (2016). Model skill scores are calculated over the 65 AERONET stations in South East Asia. The small but visible reduction in bias and of root-mean square errors at all lead times is encouraging (figure 9c,d). As the 2015 Indonesian fire produced a planetary scale signal in the aerosol emissions it is worth also analyzing the global skill scores

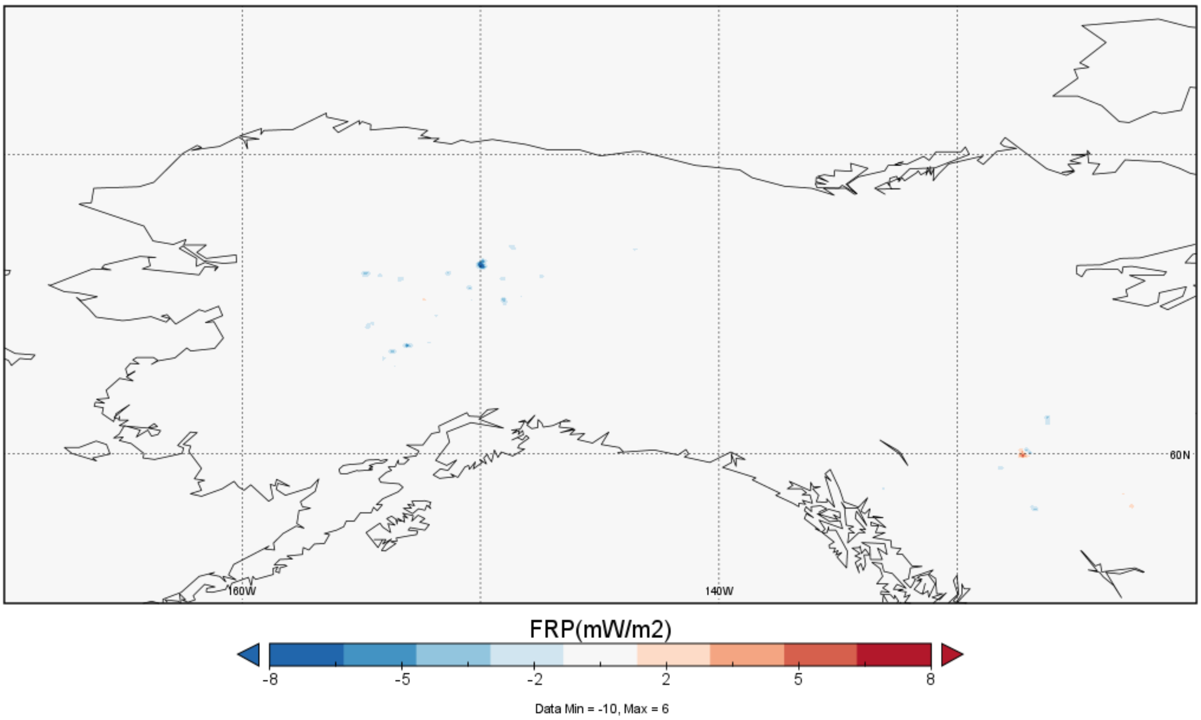

Figure 5: Differences in Fire Radiative Power from the MODIS satellite as provided by the GFAS analysis at t_0+48h forecast and t_0, where t_0 is the 07 of July 2015. A negative increment marks a decrease in fire activity.

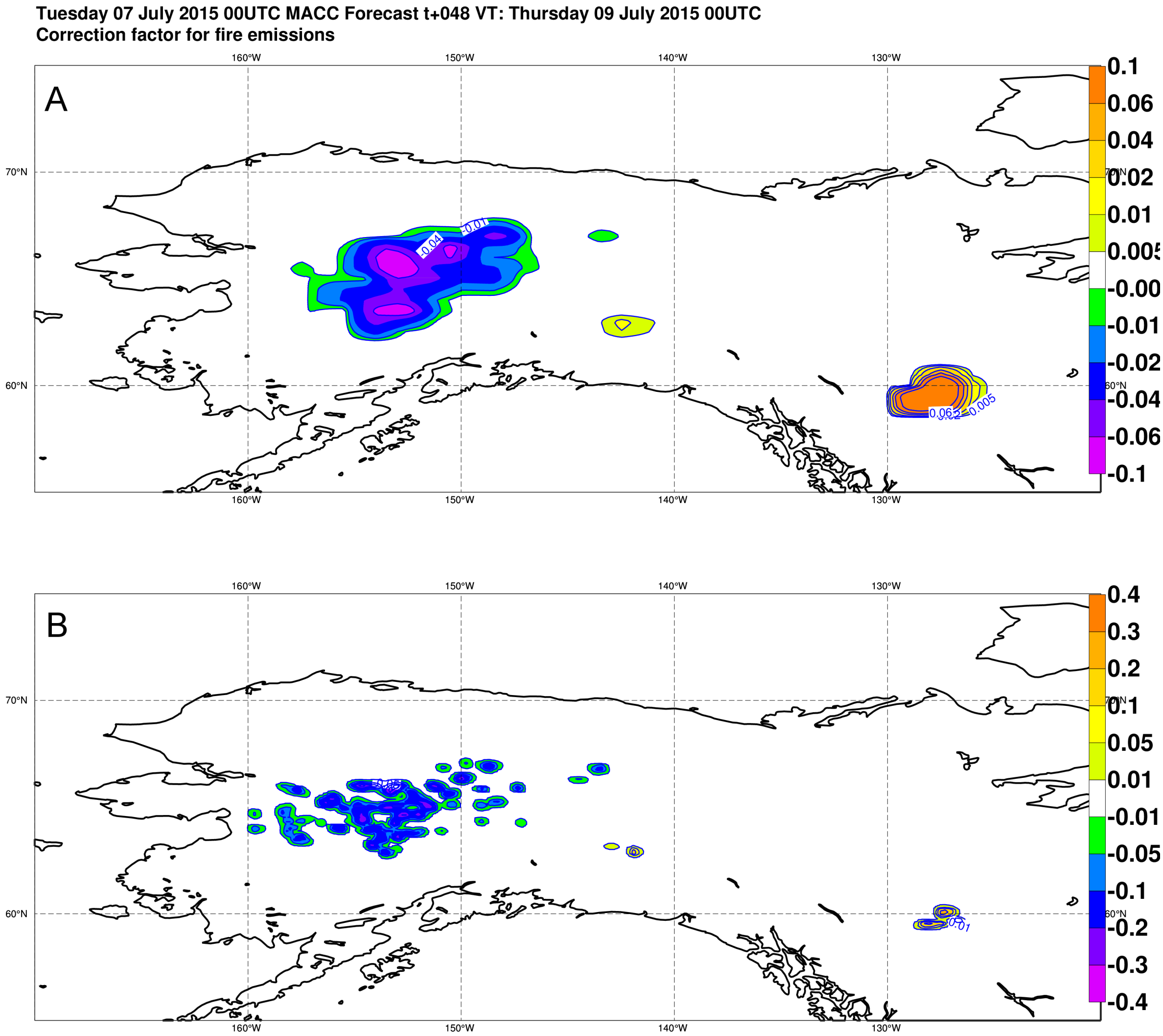

Figure 6: Modulation factor increment between t_0+48h forecast and t_0, where t_0 is the 7 of July 2016. A negative increment corresponds to a prediction for a decrease in fire activity.

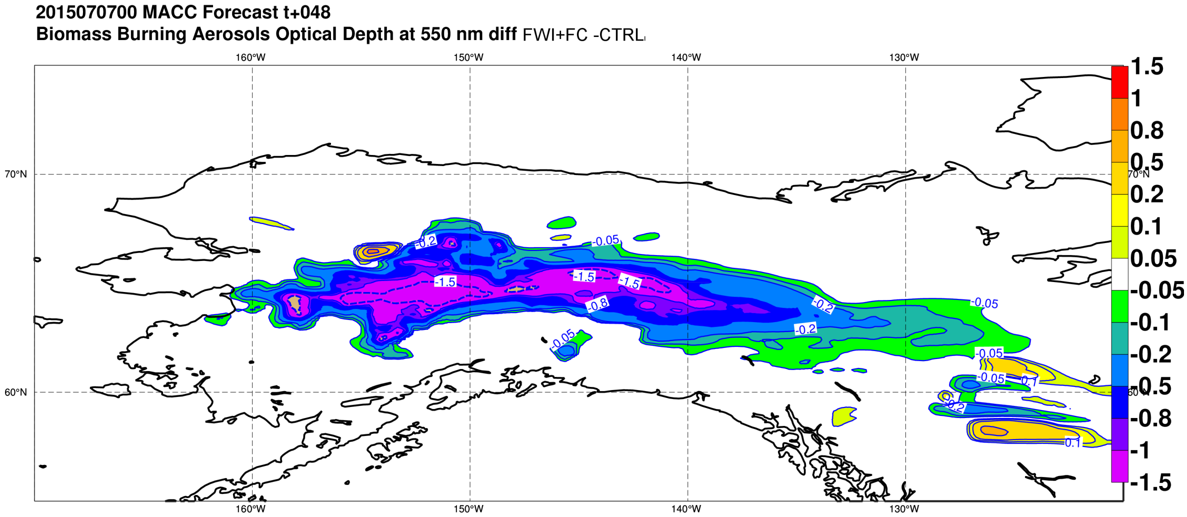

Figure 7: Differences in the forecasted aerosol load between the FWI experiment and the operational CAMS set-up (CTRL). A negative increment corresponds to a prediction for a decrease in aerosol.

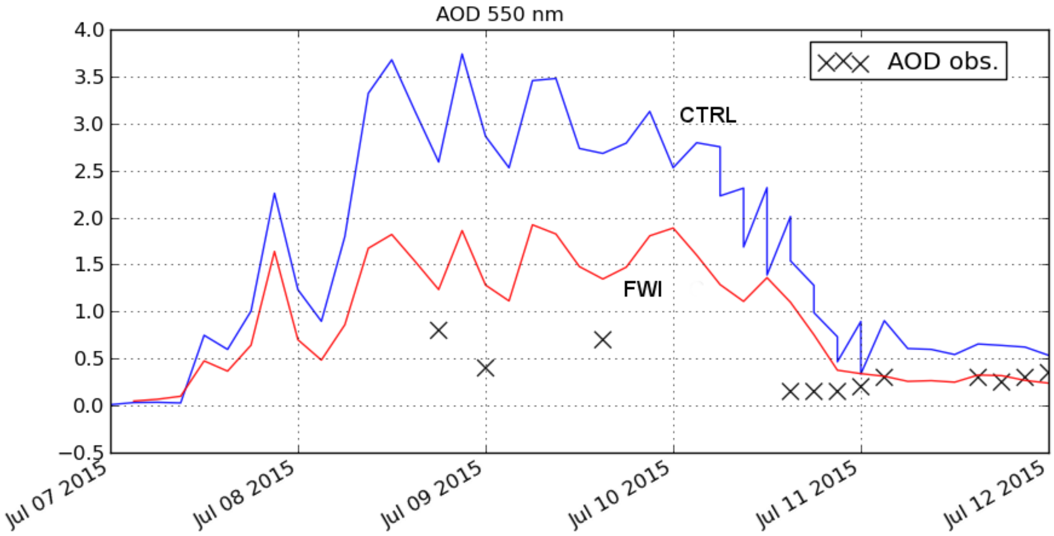

Figure 8: Aerosol optical depth (AOD) forecast interpolated to the AERONET station of Bonanza Creek [lon= -142.379W; lat=64.997N]. The interpolation is performed to the nearest grid point. The few available observations highlight a decrease in fire activity which is well forecasted by the introduction of the new modulation factor.

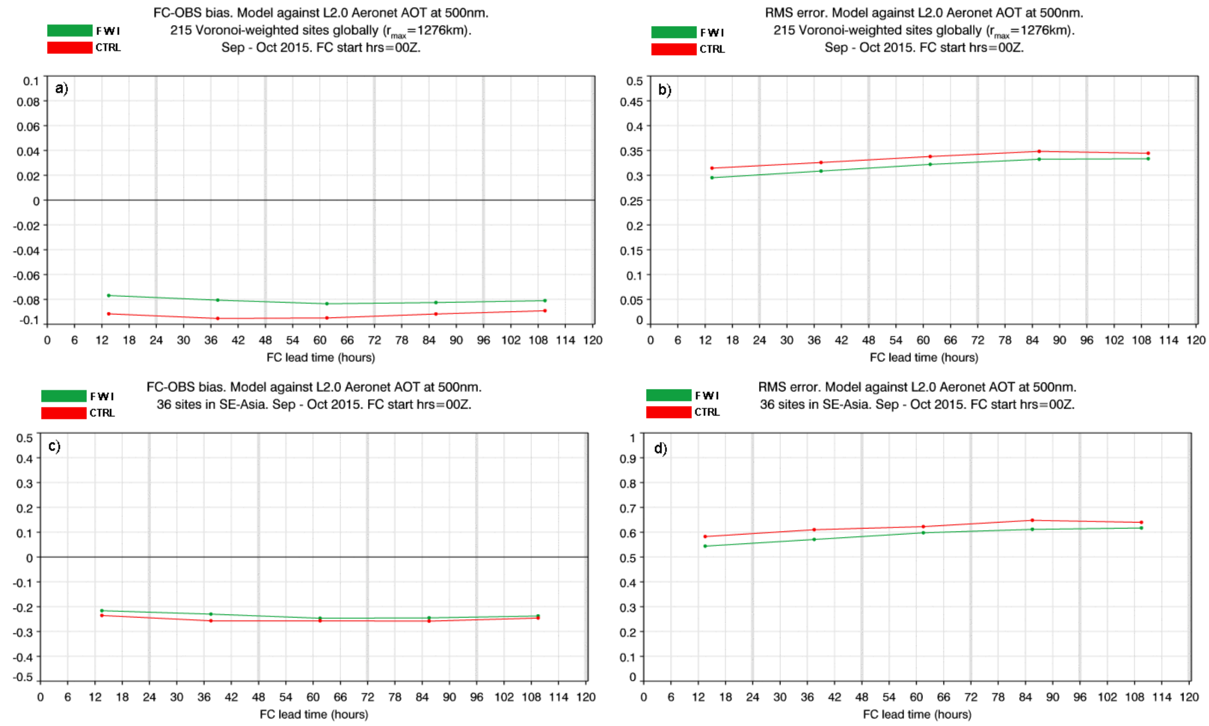

Figure 9: Bias (upper panels) and root-mean square error (lower panels) for the CAMS AOD predictions compared to the 215 and 65 AERONET stations covering the globe (panel a,b) and South East Asia only (panel c,d). The averaging period covers 2 months of simulations during the 2015 Indonesian fire. The FWI experiment is compared to the operational CAMS simulations. Only the standard CAMS resolution is shown (low resolution experiment)

using measurements from all the 215 AERONET stations over the period 1 September to 1 November. The reduction in model biases and root-mean square error is a very good indication of the improved performance of the model when fire emissions are modulated accordingly to weather conditions. The improvement is less pronounced even if still significant in the high resolution experiments (not shown).

4.3 Comparison with reanalysis

Verification is performed against the global AERONET network (figure 10). Only the first 24 hours of forecast were used in the comparison. The reanalysis bias is, as expected, substantially smaller than the operational forecast since AOD observations are assimilated during the 24 hours. The remaining bias represents the uncertainty due to the model component. The operational forecast, CTRL, displays a persistent negative bias which is constantly improved by the introduction of the new scheme. Also the root mean square error (RMS) is in general improved with the introduction of the new FWI scheme.

5 Summary

There are several studies showing the difficulties to estimate fire emissions starting from fire detection. For example French et al. (2011) and French et al. (2014) show how fuel consumption is dependent on fuel moisture and how this is mostly controlled by weather. Not including the influence of atmospheric condition on fire burning produces large errors in the estimation of the associated emission.

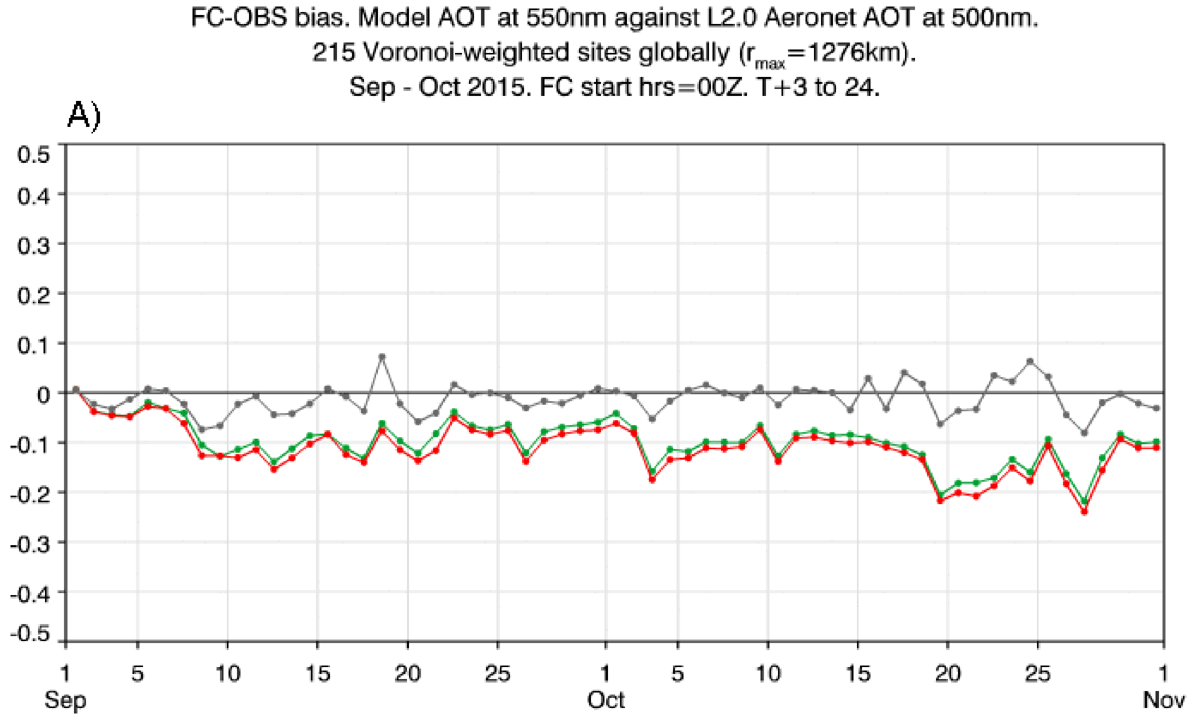

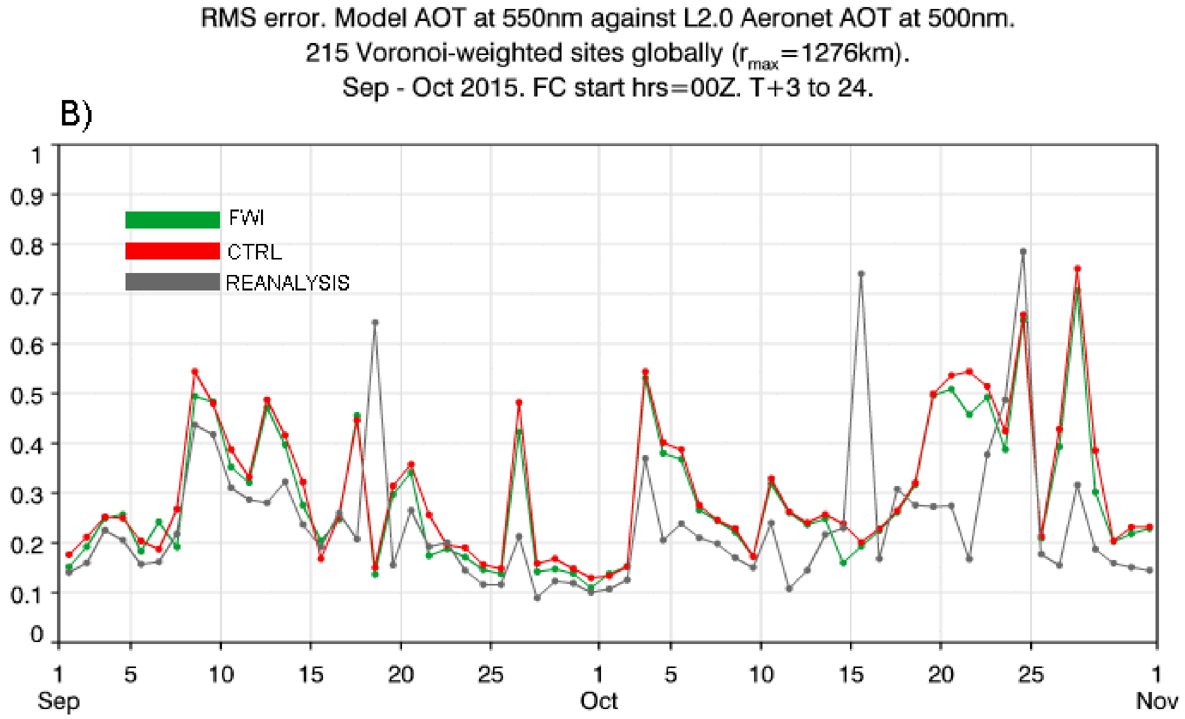

Figure 10: Daily skill scores for the FWI, CTRL and reanalysis datasets spanning September- October 2015. The verification uses the first 24h forecast for all the experiments. In the reanalysis, AOD observations are assimilated.

This study has explored a simple way to include the effect of weather on the fuel combustion by using changes in FWI to predict changes in the aerosols emissions from fires during the forecast. The differences between the operational forecast produced by the atmospheric composition model operated by the CAMS, which uses persistence of the fire contribution observed at the beginning of the forecast, with the new schemes, indicated that FWI is a good predictor for fire intensity. It also provides a good metric to reduce or enhance emissions with lead times up to five days.

A statistical analysis was performed for the Indonesian fires in 2015 which were extremely long lived (September-November) and geographically extent due to a strong ENSO. The calculation of mean model biases and root mean square errors against the Southeast Asia AERONET stations and even the global AERONET network showed a small but positive benefit provided by the introduction of the FWI modulation factor at all lead times. However, even if this new approach is thought to be an improvement over persistence, it has to be stressed that it is still a simplification compared to the use of a fire predictive model which could include interactive processes between vegetation, fuel and weather.

References

Benedetti, A., F. Di Giuseppe, J. Flemming, A. Inness, M. Parrington, S. Rmy, and J. Ziemke, 2016: Atmospheric composition changes due to the extreme 2015 indonesian fire season triggered by el niño. *BAMS*, **State of the Climate 2015 (3)**, Side–bar 2.2.

Buizza, R., M. Milleer, and T. Palmer, 1999: Stochastic representation of model uncertainties in the ecmwf ensemble prediction system. *Quarterly Journal of the Royal Meteorological Society*, **125 (560)**, 2887–2908.

Crutzen, P. J., L. E. Heidt, J. P. Krasnec, W. H. Pollock, and W. Seiler, 1979: Biomass burning as a source of atmospheric gases co, h2, n2o, no, ch3cl and cos. *Nature*, **282**, 253–256.

Cruz, M., and M. Plucinski, 2007: Billo road firereport on fire behaviour phenomena and suppression activities. *Bushfire Cooperative Research Centre, Report No. A*, **7**.

De Groot, W. J., and Coauthors, 2007: Estimating direct carbon emissions from canadian wildland fires. *International Journal of Wildland Fire*, **16 (5)**, 593–606.

Deeter, M., and Coauthors, 2003: Operational carbon monoxide retrieval algorithm and selected results for the mopitt instrument. *Journal of Geophysical Research: Atmospheres*, **108 (D14)**.

Di Giuseppe, F., F. Pappenberger, F. Wetterhall, B. Krzeminski, A. Camia, G. Libertá, and J. San Miguel, 2016: The potential predictability of fire danger provided by numerical weather prediction. *Journal of Applied Meteorology and Climatology*, **55 (11)**, 2469–2491.

Field, R. D., G. R. van der Werf, and S. S. Shen, 2009: Human amplification of drought-induced biomass burning in indonesia since 1960. *Nature Geoscience*, **2 (3)**, 185–188.

Flannigan, M. D., M. A. Krawchuk, W. J. de Groot, B. M. Wotton, and L. M. Gowman, 2009: Implications of changing climate for global wildland fire. *International journal of wildland fire*, **18 (5)**, 483–507.

Flemming, J., and Coauthors, 2015: Tropospheric chemistry in the integrated forecasting system of ecmwf. *Geoscientific model development*, **8 (6)**, 975–1003, doi:doi:10.5194/gmd-8-975-2015.

Flemming, J., and Coauthors, 2017: The cams interim reanalysis of carbon monoxide, ozone and aerosol for 2003–2015. *Atmospheric Chemistry and Physics*, **17 (3)**, 1945–1983.

French, N. H., and Coauthors, 2011: Model comparisons for estimating carbon emissions from north american wildland fire. *Journal of Geophysical Research: Biogeosciences*, **116 (G4)**.

French, N. H., and Coauthors, 2014: Modeling regional-scale wildland fire emissions with the wildland fire emissions information system*. *Earth Interactions*, **18 (16)**, 1–26.

Heil, A., J. W. Kaiser, G. R. van der Werf, M. J. Wooster, M. G. Schultz, and H. D. van der Gon, 2010: *Assessment of the real-time fire emissions (GFASv0) by MACC*. Tech. Memo 628. European Centre for Medium-Range Weather Forecasts.

Holben, B., and Coauthors, 1998: Aeroneta federated instrument network and data archive for aerosol characterization. *Remote sensing of environment*, **66 (1)**, 1–16.

Kaiser, J., and Coauthors, 2012: Biomass burning emissions estimated with a global fire assimilation system based on observed fire radiative power. *Biogeosciences*, **9 (1)**, 527–554.

Kaufman, Y., C. Ichoku, L. Giglio, S. Korontzi, D. Chu, W. Hao, R.-R. Li, and C. Justice, 2003: Fire and smoke observed from the earth observing system modis instrument-products, validation, and operational use. *International Journal of Remote Sensing*, **24 (8)**, 1765–1781.

Marlier, M. E., R. S. DeFries, A. Voulgarakis, P. L. Kinney, J. T. Randerson, D. T. Shindell, Y. Chen, and G. Faluvegi, 2013: El nino and health risks from landscape fire emissions in southeast asia. *Nature climate change*, **3 (2)**, 131–136.

Rémy, S., and Coauthors, 2017: Two global data sets of daily fire emission injection heights since 2003. *Atmospheric Chemistry and Physics*, **17 (4)**, 2921–2942.

Spessa, A., and Coauthors, 2015: Seasonal forecasting of fire over kalimantan, indonesia. *Natural Hazards and Earth System Science*, **15 (3)**, 429–442.

Stocks, B. J., T. Lynham, B. Lawson, M. Alexander, C. Van Wagner, R. McAlpine, and D. Dube, 1989: Canadian forest fire danger rating system: an overview. *The Forestry Chronicle*, **65 (4)**, 258–265.

Taylor, S. W., and M. E. Alexander, 2006: Science, technology, and human factors in fire danger rating: the canadian experience. *International Journal of Wildland Fire*, **15 (1)**, 121–135.

Van Wagner, C., 1985: Equations and fortran program for the canadian forest fire weather index system. Tech. rep., Service canadien des forets, Gouvernement du Canada.

Van Wagner, C., P. Forest, and Coauthors, 1987: Development and structure of the canadian forest fireweather index system. *Can. For. Serv., Forestry Tech. Rep*, Citeseer.

Van Wagner, C. E., and Coauthors, 1974: *Structure of the Canadian forest fire weather index*. Environment Canada, Forestry Service.

Wang, Y., R. D. Field, and O. Roswintiarti, 2004: Trends in atmospheric haze induced by peat fires in sumatra island, indonesia and el niño phenomenon from 1973 to 2003. *Geophysical research letters*, **31 (4)**.

Wooster, M. J., G. Roberts, G. Perry, and Y. Kaufman, 2005: Retrieval of biomass combustion rates and totals from fire radiative power observations: Frp derivation and calibration relationships between biomass consumption and fire radiative energy release. *Journal of Geophysical Research: Atmospheres (1984–2012)*, **110 (D24)**.